by M. Büttiker

Coherent and sequential tunneling in series barriers

A simple approach which can describe both coherent tunneling and sequential tunneling is applied to resonant tunneling through a double-barrier structure. This approach models phase-randomizing events by connecting to the conductor a side branch leading away from the conductor to a reservoir. The reservoir does not draw or supply a net current, but permits inelastic events and phase randomization. A conductance formula is obtained which contains contributions due to both coherent and sequential tunneling. We discuss the limiting regimes of completely coherent tunneling and completely incoherent transmission, and discuss the continuous transition between the two. Over a wide range of inelastic scattering times tunneling is sequential. The effect of inelastic events on the peak-to-valley ratio and the density of states in the resonant well is investigated. We also present an analytic discussion of the maximum peak conductance e/h of an isolated resonance in a many-channel conductor.

1. Introduction

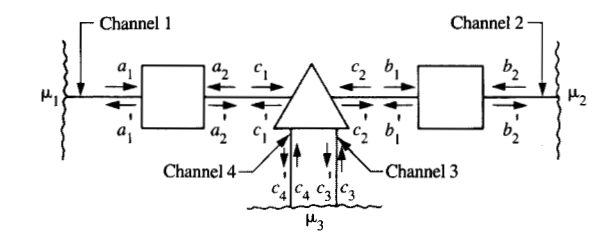
As is well known, the scattering of waves or carriers at a target which permits inelastic events in addition to elastic

[®]Copyright 1988 by International Business Machines Corporation. Copying in printed form for private use is permitted without payment of royalty provided that (1) each reproduction is done without alteration and (2) the *Journal* reference and IBM copyright notice are included on the first page. The title and abstract, but no other portions, of this paper may be copied or distributed royalty free without further permission by computer-based and other information-service systems. Permission to *republish* any other portion of this paper must be obtained from the Editor.

scattering exhibits a cross section consisting of two contributions: an elastic, coherent part and an inelastic, incoherent part [1, 2]. If for the purpose of calculating the conductance we view the conductor (or a device) as a target at which carriers are either reflected or permitted to traverse, we can similarly expect that the conductance also exhibits two contributions: a coherent contribution which arises from carriers traversing the sample suffering only elastic events, and an incoherent contribution due to carriers which suffered inelastic events while traversing the sample. Carriers which are scattered elastically emerge with a phase which has a definite relationship to the phase of the incident carriers. Carriers which are scattered inelastically emerge from the sample with a phase which is unrelated to that of the incident carriers. A discussion of conductance which views the sample as a target has long been advocated by Landauer [3, 4]. The incident currents are specified and the net current and the piled-up charges are obtained from the wavefunctions [3, 4]. This approach is typically restricted to the case of elastic scattering (coherent tunneling) only. Recently we have expanded this approach and have found an expression for the conductance which allows for both coherent and incoherent scattering processes [5]. The total transmission probability for a carrier to traverse the sample

$$T_{\text{tot}} = T_{\text{c}} + T_{\text{i}},\tag{1}$$

where $T_{\rm c}$ is the probability for a carrier to traverse the sample coherently and $T_{\rm i}$ is the transmission probability for carriers which have suffered an inelastic event. The coherent transmission probability cannot be calculated as if there were no inelastic events in the sample, since it is also affected by



Figure

Double barrier (rectangles) with an inelastic scatterer in the well, modeled by an extra branch leading away from the conductor and connected to an extra reservoir 3. Reservoirs 1 and 2 serve as source and sink of carriers and energy. Reservoir 3 draws no net current but permits inelastic phase-randomizing events. A carrier which traverses the double barrier from reservoir 1 to reservoir 2 without entering reservoir 3 is said to tunnel coherently. A carrier which progresses from reservoir 1 to reservoir 2 via reservoir 3 is said to tunnel sequentially.

the presence of these processes. For the case of a single inelastic scatterer located in the sample, the incoherent transmission probability in Equation (1) is of the form [5]

$$T_{\rm i} = \frac{S_{\rm b}S_{\rm f}}{S_{\rm b} + S_{\rm f}}.$$
 (2)

 S_b is the transmission probability for a carrier emerging from the inelastic scatterer to traverse the sample backward against the direction of carrier flow. S_f is the transmission probability for a carrier emerging from the inelastic scatterer to traverse the sample forward in the direction of current flow. Equation (2) can be understood in the following way [4]: Only a fraction $S_f/(S_f + S_b)$ of the carriers reaching the inelastic scatterer will leave the sample in the forward direction. The probability for carriers incident on the sample to reach the inelastic scatterer is S_b , and the probability for incoherent transmission is thus S_b multiplied by the factor we have just discussed. A mathematical derivation of Equation (2) is given in [5] and in Appendix A of this paper.

It is the purpose of this paper to apply Equations (1) and (2) to a sequence of two barriers with a resonant well between them [6]. Resonant tunneling is of interest in double-barrier diodes [7–15], in tunneling through a barrier with impurity states [16–17], in strongly localized conductors [18–20], and also in scanning tunneling microscopy, where a localized state can be provided by a protruding adatom [21]. In particular we investigate the effect of inelastic events on tunneling. A carrier which traverses one of the barriers coherently but is scattered inelastically in the well and loses phase memory before eventually escaping from the well is said to tunnel

sequentially [10]. A recent discussion of sequential tunneling which does not include a phase-randomizing agent found that coherent resonant tunneling and sequential tunneling lead to equivalent results for the current [14]. The analysis presented here does not support this conclusion. Coherent tunneling is contained in the first term of Equation (1), and sequential tunneling is given by the second term of Equation (1). Inelastic events which are needed to destroy phase coherence lead to a broadening and decrease of the resonant transmission [1, 2, 19] and, equivalently, to broadening of the density of states in the well. The decrease of the peak transmission with increasing inelastic scattering is accompanied by an increase of the off-resonant transmission. As a consequence the peak-to-valley ratio of the total transmission probability decreases with an increasing number of sequential processes.

To model inelastic events we use the approach of [5]. Consider Figure 1, which shows two barriers (indicated by squares) connected by pieces of perfect conductor (solid lines). The conductor is via a junction (the triangle in Figure 1) connected to a side branch. For simplicity the perfect conductors (denoted as channel 1 and channel 2 in Figure 1) are assumed to be one-dimensional, with two states only at the Fermi energy. The side branch, however, consists of two quantum channels (channels 3 and 4) and is, in turn, connected to a reservoir at a chemical potential μ_3 . Reservoir 1, at a chemical potential μ_1 , plays the role of a carrier source, and reservoir 2, at a chemical potential μ_2 , acts as a sink. Reservoir 3, in contrast, draws or delivers no net current. The condition of zero net current in the side branch leading away from the conductor determines the chemical potential μ_3 as a function of μ_1 and μ_2 [see Equation (A11)]. Each of the reservoirs has the property that it absorbs carriers incident from the conductor, regardless of the energy and the phase of the carriers. Furthermore, each reservoir emits carriers into the adjacent conductor up to its chemical potential. These rules, therefore, specify the currents incident into the conductor [3, 4]. The triangle in Figure 1 represents a quantum-mechanical junction between the side branch and the conductor. A specific example is discussed and solved in Appendix B.

A carrier scattered from the conductor into the side branch propagates to reservoir 3, where the carrier suffers inelastic events. Eventually, to maintain zero net current, reservoir 3 emits a carrier toward the junction, where the carrier is either reflected back to the reservoir or is scattered into the conductor. $S_{\rm f}$ introduced in Equation (2) is the total probability for a carrier emitted by reservoir 3 to traverse into reservoir 2. Similarly, $S_{\rm b}$ is the total probability for a carrier emitted by reservoir 3 to end up in reservoir 1. Therefore, the carriers which traverse the sample sequentially are those that are scattered into reservoir 3 and re-emitted by reservoir 3. The junction (triangle) also allows for carriers incident in the conductor to be scattered not into

the side branch but again into the conductor. Therefore, a fraction of the carriers can traverse the sample from reservoir 1 to reservoir 2 without visiting reservoir 3, and these are the carriers which traverse the sample coherently.

Let us introduce the probability ε for a carrier approaching the junction to be scattered into the side branch (channels 3 and 4). For $\varepsilon = 0$ the conductor and the side branch are completely disconnected. For $\varepsilon = 1$ every carrier incident from the conductor on the junction is transferred into the side branch and reaches reservoir 3. Thus $\varepsilon = 0$ is the case of completely coherent transmission, and $\varepsilon = 1$ is the case of completely incoherent transmission. If ε differs from these limiting values, we have both coherent transmission and sequential transmission. Thus the parameter ε determines the amount of inelastic scattering. The approach discussed here and in [5] allows the study of the continuous transition from completely coherent to completely incoherent transmission. To achieve complete phase randomization, carriers need to be scattered with probability 1 into reservoir 3. If the junction is required to be symmetric with respect to right- and left-moving carriers, probability 1 can only be obtained if the side branch contains two channels. If the side branch contains only one channel and is symmetric with respect to right- and left-moving carriers, the maximum probability [5] which can be achieved for scattering into reservoir 3 is 1/2.

The method of introducing inelastic scattering or sequential processes described above is not limited to a single side branch. Conductors connected to many side branches are of interest as well [5, 22]. Another system is obtained if we eliminate two of the reservoirs in Figure 1 by forming the conductor into a loop. A normal loop, driven by a magnetic flux and with a single side branch to model the effect of inelastic events on coherent superconducting-like phenomena [23], is the subject of [24]. Another interesting feature of the approach proposed here is the following: The conductor shown in Figure 1 is a three-terminal device. Reservoir 1 can serve as a current source and reservoir 3 as a current sink. This situation bears a close resemblance to the experiment of Morkoc et al. [25], where current was drawn directly from the "well." As in the experiment [25], our approach also yields a resonant conductance in this case, even though a net current flows only through one barrier.

Below, we emphasize the two-terminal conductance [26] $\mathcal{G} = \mathcal{R}^{-1} = (e^2/\hbar)T_{\rm tot}$ considering channels 1 and 2 as the conductor. Thus we are not directly addressing the negative differential conductance phenomena which were first discussed by Tsu and Esaki [7] and which have generated much interest lately [8–15, 25]. Instead, we assume that we can control the Fermi energy and that it is the dependence of the conductance on the Fermi energy which matters. This paper is also limited to the case where kT is small compared to the width of the resonance (see, however, Appendix A). Most of the calculations leading to the results presented

below are relegated to four appendices. We focus on onedimensional conductors, except in Appendix C, where we discuss the peak conductance due to an isolated resonant state in a many-channel conductor.

2. Completely coherent versus completely incoherent transmission

In this section we discuss the extreme limits in which one of the terms in Equation (1) vanishes. In the completely coherent limit $T_i = 0$, the coherent transmission probability through two barriers in series exhibits resonances near the energies of the quasi-eigenstates of the well,

$$T_{\rm c} = T_{\rm res} \frac{\frac{1}{4} \Gamma_{\rm e}^2}{(E - E_{\rm e})^2 + \frac{1}{4} \Gamma_{\rm e}^2},\tag{3}$$

with a peak value at resonance

$$T_{\rm res} = \frac{4T_1 T_2}{\left(T_1 + T_2\right)^2}. (4)$$

The peak value is 1 if the transmission probabilities of the two barriers are equal, and is smaller than 1 and given by $T_{\rm res} \simeq 4T_1/T_2$ in the case that $T_1 \ll T_2$. In Equation (3),

$$\Gamma_{\epsilon} = \Gamma_{1} + \Gamma_{2} \tag{5}$$

is the total elastic width; Γ_1 and Γ_2 are the partial elastic widths of the resonant level. $1/\tau_e = \Gamma_e/\hbar$ is the decay rate of the resonant state. The transmission through a double-barrier structure is analyzed in Appendix B. This calculation, which invokes some simplifying assumptions not relevant for our subsequent discussion, yields for the partial elastic widths the WKB expressions

$$\Gamma_1 = \hbar \nu T_1, \qquad \Gamma_2 = \hbar \nu T_2. \tag{6}$$

Here ν is an attempt frequency, and in the case of a square well is given by $\nu = 2w/v$, where w is the width of the well and v is the velocity of a carrier in the well at the resonant energy E_r . At energies E away from E_r , transmission is still coherent but typically many orders of magnitude smaller than $T_{\rm res}$, and, approximately,

$$T_{\rm c} = T_{\rm off} \propto \frac{1}{4} T_1 T_2. \tag{7}$$

Therefore, the peak-to-valley ratio $T_{\rm res}/T_{\rm off}$ is exponentially large if the transmission probabilities are exponentially small. Such huge peak-to-valley ratios have not been observed experimentally; inelastic scattering, discussed below, is one reason for this discrepancy. But there are other reasons also, e.g., the averaging over an energy range due to a three-dimensional incident distribution [10], deviations from an ideal planar structure, and elastic scattering due to impurities [15].

Let us now turn away from the limit of completely coherent transmission and consider the limit of completely incoherent transmission, i.e., $T_c = 0$. In this case every carrier reaching the inelastic scatterer loses phase. In this limit a carrier cannot travel from one side of the resonant well to the other without being scattered inelastically. This process is a special limit of the sequential tunneling process and is labeled completely incoherent. In general, a sequential tunneling process permits many oscillations in the well with frequency ν before the carrier loses phase memory. We invoke a scatterer (triangle in Figure 1) which re-emits carriers with equal probability to the left and right into the conductor. In the limit of complete phase randomization, the probability of a carrier emerging from the inelastic scatterer to traverse the sample backward is given by $S_b = T_1$, and similarly the probability of a carrier being scattered in the forward direction is $S_f = T_2$. Therefore, in the completely incoherent limit Equation (2) yields [5]

$$T_{\text{tot}} = T_{\text{i}} = \frac{T_{1}T_{2}}{T_{1} + T_{2}} = \left[\frac{1}{T_{1}} + \frac{1}{T_{2}}\right]^{-1}.$$
 (8)

A single barrier with transmission probability T_i in an otherwise perfect wire gives rise to a two-terminal resistance $\mathcal{R}_j = (\hbar/e^2)T_j^{-1}$. Therefore, Equation (8), using $\mathcal{R} = (\hbar/e^2)T_{\text{tot}}^{-1} = (\hbar/e^2)T_{\text{i}}^{-1}$, yields the series addition of resistors, $\mathcal{R} = \mathcal{R}_1 + \mathcal{R}_2$. If inelastic scattering is so strong that every carrier loses phase memory while traversing the well, the resistance of the structure contains no detailed information about the geometrical arrangements of the scatterers (separation of the barriers) but is the sum of the resistances due to the individual scatterers. Note that the transmission in the incoherent limit, Equation (8), is not the same as the off-resonant coherent transmission, Equation (8). If the transmission probabilities are small, the completely incoherent transmission probability, Equation (8), far exceeds the off-resonant coherent transmission probability, Equation (7). On the other hand, the transmission at resonance T_{res} , Equation (3), exceeds the purely sequential transmission probability, Equation (8). It is now clear what happens when we start from a situation where only coherent processes are allowed and introduce inelastic events. Both the transmission at resonance [peak value, Equation (4)] and the off-resonance transmission [minimum value, Equation (7)] must, with increasing inelastic scattering, eventually approach the completely incoherent limit, Equation (8). Therefore, the peak value must in general decrease with an increasing amount of inelastic scattering, and the off-resonant transmission must in general increase with increasing inelastic scattering.

The transition from the completely coherent limit to the completely incoherent limit occurs through the sequential tunneling regime in which carriers can execute many oscillations in the well before losing phase memory. The distinction of three regimes, the *coherent* limit, the *sequential* tunneling regime, and the *completely incoherent* limit, is made because resonant tunneling has two frequency scales

[27] which, when compared with the inelastic scattering rate Γ_i/\hbar , yield three physically distinct regimes: The time scales [2] associated with a resonance are the elastic decay rate Γ_e/\hbar given by Equations (5) and (6) and the attempt frequency $\nu = \nu/2w$. We show that for $\Gamma_i \ll \Gamma_e$ we are in a regime where the main part of the current is carried by coherent processes, in the regime $\Gamma_e \ll \Gamma_i \ll \hbar \nu$ current is carried by sequential tunneling processes, and if $\hbar \nu \ll \Gamma_i$ we are in the completely incoherent limit. Below we discuss this in more detail.

3. Crossover from coherent to sequential transmission

To study the crossover from coherent resonant tunneling to coherent sequential tunneling it is possible to apply the formulae of Breit and Wigner [1, 2]. The applicability of these formulae to tunneling through disordered conductors in the presence of inelastic scattering is mentioned by Azbel et al. [18]. However, the results presented in [18] are not compatible with the Breit and Wigner approach. Subsequently results compatible with the Breit and Wigner formulae were obtained for a symmetrical double barrier by Stone and Lee [19]. They used an imaginary (optical) potential to describe inelastic scattering. This does not allow the determination of the forward and backward scattering probabilities. Reference [19] makes the plausible assumption (for a symmetric barrier) that $S_b = S_f = S$, and consequently $T_i = S/2$. The approach of [5] introduced in Section 1 allows us to determine the forward and backward scattering rates S_h and S_f . These probabilities are also determined by the Breit and Wigner formulae, which are mentioned in textbooks [2] but seem to have found little attention in solidstate physics. A discussion of these formulae is presented in Appendix C.

The key point of Breit and Wigner [1, 2] is the notion that if there is elastic resonant transmission from channel 1 to channel 2,

$$T_{\rm c} = T_{21} = \frac{\Gamma_1 \Gamma_2}{(E - E_{\rm r})^2 + \frac{1}{4} \Gamma^2},$$
 (9)

then the weakly coupled inelastic channels (channels 3 and 4 in Figure 1) are also characterized by resonant transmission and couple to the elastic transmission with partial widths Γ_3 and Γ_4 . The backward scattering probability becomes

$$S_{\rm b} = \frac{\Gamma_1 \Gamma_{\rm i}}{(E - E_{\rm c})^2 + \frac{1}{4} \Gamma^2},\tag{10}$$

and the forward scattering probability becomes

$$S_{\rm f} = \frac{\Gamma_2 \Gamma_{\rm i}}{(E - E_{\rm r})^2 + \frac{1}{4} \Gamma^2},\tag{11}$$

where $\Gamma_i = \Gamma_3 + \Gamma_4$ is the total inelastic width. According to Breit and Wigner, the width Γ in Equations (9)–(11) is the sum of all the partial rates,

$$\Gamma = \sum_{i=1}^{j=4} \Gamma_j = \Gamma_e + \Gamma_i.$$
 (12)

 Γ_1 and Γ_2 are specified by Equation (6). For the model studied in Appendix B, the inelastic widths are

$$\Gamma_3 = \Gamma_4 = \hbar \nu \varepsilon. \tag{13}$$

Here ε is the probability for a carrier in the conductor, approaching the junction, to be scattered into the side branch [see Figure 1 and Equation (B8)]. By using Equations (10), (11), and (2), we find for the sequential transmission probability

$$T_{i} = T_{\text{res}} \frac{\frac{1}{4} \Gamma_{e} \Gamma_{i}}{(E - E_{e})^{2} + \frac{1}{4} \Gamma^{2}}.$$
 (14)

Here we have used the fact that $T_{\text{res}} = 4\Gamma_1 \Gamma_2 / \Gamma_e^2$. The total transmission probability near a resonance is thus

$$T_{\text{tot}} = T_{\text{res}} \frac{\frac{1}{4} \Gamma_{\text{c}} \Gamma}{(E - E_{\text{r}})^2 + \frac{1}{4} \Gamma^2}.$$
 (15)

Therefore, the peak value of the total transmission probability at resonance is $T_{\rm res}\Gamma_{\rm e}/\Gamma$. Thus the inclusion of inelastic or sequential events leads to a decrease of the peak value and broadens the resonance. It is interesting to compare the fraction of the current carried by the carriers traversing the structure coherently, $T_{\rm c}/T_{\rm tot}=\Gamma_{\rm e}/\Gamma$, with the fraction of the current carried by the carriers traversing the sample sequentially, $T_{\rm i}/T_{\rm tot}=\Gamma_{\rm i}/\Gamma$. To evaluate these fractions we have used Equations (1), (2), (9), and (10). We see that if the total elastic width and the total inelastic width are equal, the currents due to coherent tunneling and due to sequential tunneling are equal. The smaller the elastic width, the smaller is the amount of inelastic scattering [19] needed to make the sequential tunneling current dominant.

In the crossover region $\Gamma_e \simeq \Gamma_i$ we have not only a decrease of the peak value of the transmission with inelastic scattering, but also an increase of the off-resonance transmission probability. The model calculation in Appendix B yields an off-resonance (minimal) transmission probability

$$T_{\text{tot,off}} \propto \frac{1}{4} \frac{\Gamma}{\Gamma} T_1 T_2.$$
 (16)

Using Equations (15) and (16) yields a peak-to-valley ratio of the order

$$\frac{T_{\text{tot,res}}}{T_{\text{tot,off}}} \propto \left(\frac{\Gamma_e}{\Gamma}\right)^2 \frac{1}{\left(T_1 + T_2\right)^2} = \frac{(\hbar \nu)^2}{\Gamma^2},\tag{17}$$

where we have used Equation (5). Thus the peak-to-valley ratio of the transmission probability decreases rapidly as sequential tunneling processes become important.

We mention here an additional result which is derived in Appendix D. The density of states in the resonant well also depends on the degree of sequential tunneling. For the density of states in the well we find in the crossover region

(12)
$$\left[\frac{dN}{dE} \right] = \frac{1}{\pi} \frac{\frac{1}{2} \Gamma}{(E - E)^2 + \frac{1}{2} \Gamma^2}.$$
 (18)

Note that the density of states in the well is determined by the total width Γ , Equation (12). Thus, as the number of sequential tunneling processes increases, the density of states in the well becomes less sharply peaked at the resonant energy and broadens. Reference [14], in attempting to show that resonant tunneling and sequential tunneling are equivalent, uses a density of states which is independent of the degree of inelastic scattering.

The Breit and Wigner formalism can only handle the crossover from the coherent to the sequential tunneling regime. If the inelastic scattering rate exceeds the elastic width by orders of magnitude, one must go beyond this formalism.

4. Coherence corrections of the completely incoherent transmission

In the limit in which every carrier traversing the well is scattered inelastically, the coherent transmission probability T_c vanishes and $S_b = T_1$ and $S_f = T_2$. The total transmission probability is given by Equation (8). The completely incoherent transmission is independent of the separation w of the barriers. Consider now the situation in which a tiny fraction of all the carriers can execute one or more full revolutions in the well before losing phase memory. We can then expect a small correction of Equation (8) by a term which depends on the phase $\phi = kw$ accumulated during well traversal. This correction term is, therefore, sensitive to the geometrical arrangement of the barriers. Below we consider the case where the carriers in the well can execute at most one revolution before losing phase memory.

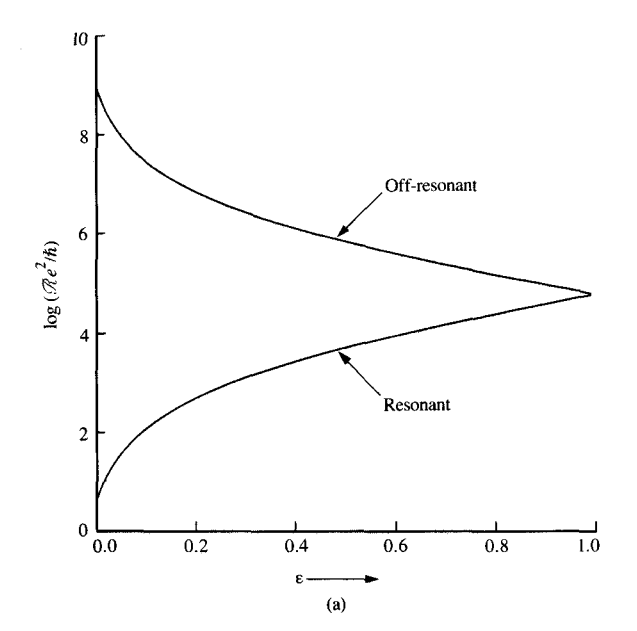
Suppose that the carriers have a small probability $1 - \varepsilon$, with ε close to 1 to traverse the well without being scattered into reservoir 3. Interestingly, to the lowest order in $1 - \varepsilon$, it is the forward and backward scattering probabilities which contain these interference terms, not the coherent transmission probability. The coherent transmission probability T_{ε} is easily obtained in this limit. The probability amplitude for traversal of the structure of Figure 1 from channel 1 to channel 2 is $t_{21} = t_1 \sqrt{1 - \varepsilon} \ t_{22}$, and hence

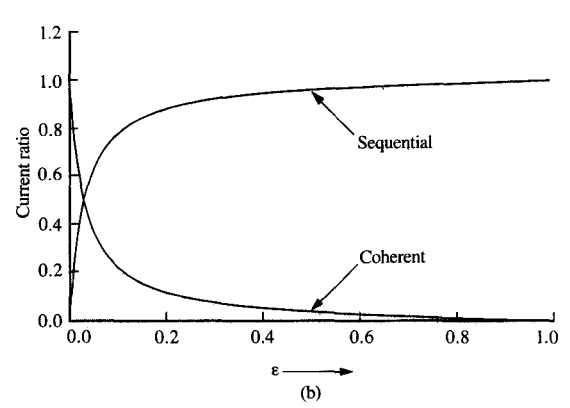
$$T_{c} = T_{21} = |t_{21}|^{2} = (1 - \varepsilon)T_{1}T_{2}.$$
 (19)

Carriers which traverse coherently from channel 1 to channel 2 and in addition execute a full revolution in the well have to traverse the well at least three times and are of order $(1 - \varepsilon)^2$.

Now consider the sequential tunneling process and let us focus on the backward scattering probability S_b . Consider the carriers which are injected by the inelastic scatterer into the conductor with a negative velocity. A fraction of these leave the well through the left barrier with amplitude t_1 and give rise to a backscattering probability $S_b = T_1$ to lowest order. Most carriers are reflected back into the well if R_1 is close to







(a) Maximum resistance and minimum resistance corresponding to off-resonant and resonant transmission of a double-barrier structure as a function of ε . The parameter ε is the probability for carriers incident on the junction to be scattered into the extra reservoir. The two barriers forming the well have transmission probability $T_1 = 0.05$ and $T_2 = 0.01$. (b) Ratio of coherent current and sequential current as a function of ε for the double-barrier structure with parameters as in Figure 2(a).

1, and a tiny fraction of these carriers traverses the well back and forth, completing a full revolution. The probability amplitude for a carrier starting in the well and completing a full revolution is $A = (\sqrt{1-\epsilon} \ R_1^{1/2})(\sqrt{1-\epsilon} \ R_2^{1/2})e^{i(2\phi+\Delta\phi)}$ Here $\sqrt{1-\epsilon}$ is the absolute value of the probability amplitude for a carrier to traverse the well without losing phase (without being scattered into reservoir 3 of Figure 1), and $R_2^{1/2}$ and $R_1^{1/2}$ are the absolute probability amplitudes for

reflection at the right and left barrier. $\phi = kw$ with w the width of the well is the phase accumulated during well traversal, and $\Delta \phi$ is the phase accumulated during the two reflection processes. The superposition of the carriers escaping directly from the well with amplitude t_1 on those that escape after one revolution with probability amplitude t_1A gives rise to a combined amplitude t_1+t_1A , and hence to an interference correction proportional to $2T_1\text{Re}[A]$, with

$$Re [A] = (1 - \varepsilon) R_1^{1/2} R_2^{1/2} \cos(2\phi + \Delta\phi).$$
 (20)

Consideration of *all* the processes that contribute to the backward-scattering probability to order $1 - \varepsilon$ gives (see also Appendix B)

$$S_{\rm b} = T_1 [1 - (1 - \varepsilon)(T_2 + 2R_1^{1/2}R_2^{1/2}\cos(\Phi))]. \tag{21}$$

Here $\Phi = 2\phi + \Delta\phi$ is the total phase. In contrast to $T_{\rm c}$, the backward-scattering probability $S_{\rm b}$ is sensitive to the separation of the two barriers. Similarly, for the forward-scattering probability we find

$$S_{\rm f} = T_2[1 - (1 - \varepsilon)(T_1 + 2R_1^{1/2}R_2^{1/2}\cos(\Phi))]. \tag{22}$$

Using Equations (19) – (22) to evaluate Equations (1) and (2) yields

$$T_{\text{tot}} = \frac{T_1 T_2}{T_1 + T_2} \left[1 + 2(1 - \epsilon)(T_1 T_2 - R_1^{1/2} R_2^{1/2} \cos(\Phi)) \right]. \tag{23}$$

For $\varepsilon = 1$, Equation (23) gives exactly the result of Equation (8) for completely incoherent transmission. Equation (23) is valid independent of the magnitude of the transmission probabilities T_1 and T_2 . If these are taken to be small compared to unity and if we use in addition Equation (B22), which expresses ε in terms of the inelastic scattering time τ_1 and the well frequency $\nu = v/2w$, Equation (23) becomes

$$T_{\text{tot}} = \frac{T_1 T_2}{T_1 + T_2} \left[1 - 2e^{-1/2\nu \tau_i} \cos(\Phi) \right]. \tag{24}$$

Thus, in the case of strong inelastic scattering $2\nu\tau_i < 1$, we obtain corrections to the completely incoherent transmission which are sensitive to the geometrical arrangement of the scatterers. If the Fermi energy is such that $\Phi = (2n+1)\pi$, we have maximum transmission, and for $\Phi = 2\pi n$ we have minimal transmission.

Due to interference effects, the number of states in the well per unit energy (see Appendix D) is also modified. In the case of complete phase randomization, the number of states per unit energy is dN/dE = 2w(dn/dE). A calculation yields

dN/dE = 2w(dn/dE)

$$\times [1 + (1/2)(1 - \varepsilon)(R_1 + R_2 - 2R_1^{1/2}R_2^{1/2}\cos(\Phi))],$$
 (25)

which in the limit of small transmission probabilities becomes

$$dN/dE = 2w(dn/dE)[1 + 2e^{-1/2\nu\tau_i}\sin^2(\Phi/2)].$$
 (26)

The enhanced transmission at $\Phi = (2n + 1)\pi$ coincides with an enhanced density of states and the minimal transmission at $\Phi = 2n\pi$ is accompanied by a reduced density of states.

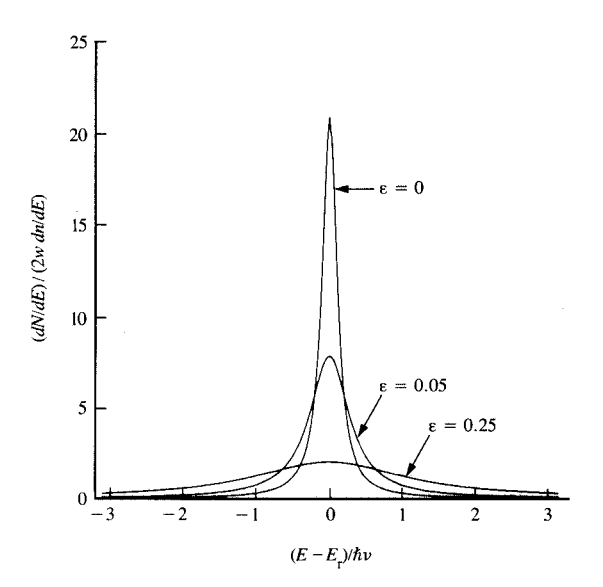
5. Transition from completely coherent to completely incoherent transmission

In Section 2 we discussed the limiting behavior of completely coherent and completely incoherent transmission. In Sections 3 and 4 we investigated the departure from these simple limits. In this section we address the transition from one limiting behavior to the other for the entire domain of inelastic scattering. A simple model calculation is presented in Appendix B, and here we summarize these results by discussing **Figures 2** and **3**.

Figure 2(a) shows the two-terminal resistance $\mathcal{R}/(\hbar/e^2) = T_{\text{tot}}^{-1}$, with T_{tot} given by Equations (1) and (2) evaluated in Appendix B for a two-barrier structure with $T_1 = 0.05$ and $T_2 = 0.01$ as a function of the coupling parameter ε . The upper curve shows the maximum resistance (minimum or off-resonant transmission) and the lower curve shows the minimum resistance (peak transmission). $\varepsilon = 0$ is the purely coherent limit, and the minimum (maximum) resistance is determined by Equations (3) and (7), respectively. $\varepsilon = 1$ is the purely incoherent limit, and the resistance is determined with the help of Equation (8). For small ε the minimum resistance is given by Equation (15) (Breit and Wigner limit) and the maximum resistance is determined by Equation (16). An increasing number of sequential tunneling processes (increasing ε) leads to a decreasing ratio of the minimum and maximum resistance (transmission) caused both by a decrease in the maximum transmission probability and by a rise in the minimum transmission probability. Thus sequential tunneling leads to lower peak values in the transmission, but increases the offresonant transmission. For ε close to 1, only small corrections remain from the completely incoherent transmission. These corrections are due to a small fraction of carriers which can undergo a complete revolution before leaving the well, as discussed in Section 4.

Figure 2(b) shows the ratio of the coherent current to the total current, $T_{\rm c}/T_{\rm tot}$, and the ratio of the current due to incoherent (sequential) processes to the total current, $T_{\rm i}/T_{\rm tot}$. For small transmission probabilities, a small amount of inelastic scattering $2\epsilon = 1/\nu \tau_{\rm i} > (T_1 + T_2) = 1/\nu \tau_{\rm e}$ makes the sequential current dominant.

The density of states in the well gives a good indication of the degree to which coherence effects play a role. In Figure 3 the density of states in the well (calculated in Appendix C) is shown as a function of $E-E_{\rm r}$ for three different scattering rates. For small scattering rates Equation (16) applies. With increasing inelastic scattering, the variation in the density of states is less pronounced. For $\varepsilon=1$, i.e., when carriers are scattered every time they reach the junction in Figure 1, the density of states in the well is without structure.



Floure 3

Number of states per unit energy in the resonant well for three different degrees of inelastic scattering as a function of energy. E_r is the resonant energy and v is the well frequency; (dn/dE) is the density of states in the perfect conductors and w is the well width.

Phase randomization is a consequence of inelastic events. To describe such processes it is necessary to explicitly take into account the phase-randomizing agent. To describe sequential tunneling in terms of a density of states corresponding to the completely coherent case, as in [14], is not correct. In order to have sequential tunneling we must have a phase-randomizing scatterer, and this in turn affects the density of states.

Admittedly, in this paper we have focused on a onedimensional (one quantum channel) conduction problem, and inelastic scattering might have a more drastic effect in such small systems. The approach introduced here can, however, be extended to treat more complex situations, as indicated in Appendix C.

Note added in proof

References [14] and [34] consider a large applied voltage V which exceeds the width Γ of the resonance. References [14] and [34] find an integrated current which is independent of the inelastic width Γ_i , when the resonance is centered in the applied bias range. We emphasize that Equation (15) has a limited range of validity. For an applied voltage large compared to the elastic width Γ_e but small compared to $h\nu$, the current decreases with increasing elastic width Γ_i with a slope

$$-\frac{\partial}{\partial \Gamma_{i}} \log I \cong \frac{1}{eV} \ge \frac{1}{\hbar \nu}. \tag{27}$$

Equation (27) is valid for a small inelastic width. The peak-to-valley ratio is smaller than that given by Equation (17) and is proportional to $\hbar^2 \nu^2 / \Gamma V$.

Acknowledgment

I thank R. Landauer for valuable comments, and am also grateful for discussions with N. D. Lang, P. Marcus, E. Mendez, P. Price, and H. Thomas.

Appendix A: Coherent and sequential parts of conductance

Consider the conductor [5] in Figure 1. To derive Equations (1) and (2) we have to calculate the net current which flows due to a difference in the chemical potentials μ_1 and μ_2 . The perfect conductors between the reservoir and the scatterers are assumed to be one-dimensional; i.e., there are two states at the Fermi energy, one with positive velocity (from the reservoir toward the conductor) and one with negative velocity. Let us consider the case of a low temperature such that the energy spread kT can be neglected. The reservoir jfeeds all channels connected to it equally [29] and up to the chemical potential μ_r . Let us introduce a reference potential μ_0 which is smaller than or equal to the lowest of the three chemical potentials μ_1 , μ_2 , μ_3 . Below the reference potential μ_0 all states are completely filled and we need to consider only the energy range above μ_0 . The current emitted by the reservoir j into an adjacent channel in the energy range μ_i –

$$I_{in} = ev(dn/dE)(\mu_i - \mu_0). \tag{A1}$$

Here v is the Fermi velocity and dn/dE is the density of states (for one spin direction). In one dimension $dn/dE = (dn/dk)(dk/dE) = 1/2\pi\hbar v$, since $dn/dk = 1/2\pi$. Thus the reservoir injects into each channel connected to it a current

$$I_{\rm in} = (e/2\pi\hbar)(\mu_i - \mu_0).$$
 (A2)

To obtain the net currents we must specify the probabilities of carriers for transmission and reflection at the conductor of Figure 1. Let T_{kl} be the probability for a carrier incident in channel l to traverse the structure into channel k to reach a different reservoir. The probabilities for a carrier emitted by a reservoir to be scattered back into the same reservoir are denoted by R_{kl} . In the absence of a magnetic field the probabilities are symmetric, $T_{kl} = T_{lk}$, $R_{kl} = R_{lk}$. Furthermore, because of current observation,

$$R_{11} + T_{12} + T_{13} + T_{14} = 1,$$
 (A3a)

$$T_{21} + R_{22} + T_{23} + T_{24} = 1,$$
 (A3b)

$$T_{31} + T_{32} + R_{33} + R_{34} = 1,$$
 (A3c)

$$T_{41} + T_{42} + R_{43} + R_{44} = 1.$$
 (A3d)

Consider now the net current flowing in channel 1. In channel 1, reservoir 1 contributes a net current

 $(e/2\pi\hbar)(1-R_{11})(\mu_1-\mu_0)$. The incident current given by Equation (A2) is diminished by reflection at the sample. Current injected by reservoir 2 gives rise to a current $-(e/2\pi\hbar)T_{12}(\mu_2-\mu_0)$ in channel 1. Current injected by reservoir 3 into channels 3 and 4 gives rise to a current $-(e/2\pi\hbar)(T_{13}+T_{14})(\mu_3-\mu_0)$ in channel 1. Collecting all contributions yields a net current in channel 1,

$$I_1 = \frac{e}{2\pi\hbar} \left[(1 - R_{11})\mu_1 - T_{12}\mu_2 - S_b\mu_3 \right]. \tag{A4}$$

Here we have introduced the total transmission probability

$$S_{\rm b} = T_{13} + T_{14} \tag{A5}$$

for a carrier incident in channel 3 or 4 to be scattered into channel 1. The reference chemical potential does not occur in Equation (A4) since the currents proportional to μ_0 add to zero because of Equation (A3a). Similar considerations yield a current in channel 2 given by

$$I_2 = \frac{e}{2\pi\hbar} \left[(1 - R_{22})\mu_2 - T_{21}\mu_1 - S_f\mu_3 \right],\tag{A6}$$

where

$$S_{\rm f} = T_{23} + T_{24} \tag{A7}$$

is the total probability for carriers incident in channels 3 and 4 to be scattered into channel 2. Finally, the currents in channels 3 and 4 are found to be

(A1)
$$I_3 = \frac{e}{2\pi\hbar} \left[(1 - R_{33} - R_{34})\mu_3 - T_{31}\mu_1 - T_{32}\mu_2 \right],$$
 (A8)

$$I_4 = \frac{e}{2\pi h} \left[(1 - R_{44} - R_{43})\mu_3 - T_{41}\mu_1 - T_{42}\mu_2 \right]. \tag{A9}$$

The net current flow in the extra branch consisting of channels 3 and 4 has to be zero. Using Equations (A3) and the definition equations (A5) and (A7), we find

$$0 = I_3 + I_4 = \frac{e}{2\pi\hbar} \left[(S_f + S_b)\mu_3 - S_b\mu_1 - S_f\mu_2 \right], \tag{A10}$$

and hence the chemical potential μ_3 is given by [5]

$$\mu_3 = \frac{S_b \mu_1 + S_f \mu_2}{S_b + S_f}.$$
(A11)

Equation (A11) is a result which is important beyond the context of this paper. The extra branch leading away from the conductor and connected to the reservoir also can describe a voltage probe, and μ_3 is the chemical potential which is measured at this probe [28]. Equation (A11) generalizes earlier concepts of "potentiometers" used in [29–31] because it invokes no assumptions on the symmetry of the coupling between the lead and the conductor and because the junction in Figure 1 is treated fully quantum-mechanically; i.e., amplitudes are matched, and not intensities.

Here we use Equation (A11) to eliminate μ_3 from Equation (A4) or Equation (A6) to determine the net current flow along the conductor. Current conservation requires $I = I_1 = -I_2$. Using Equation (A3) and the symmetry $T_{ij} = T_{ji}$ yields, after a little algebra,

$$I = \frac{e}{2\pi\hbar} \left(T_{\rm c} + \frac{S_{\rm b}S_{\rm f}}{S_{\rm b} + S_{\rm f}} \right) (\mu_1 - \mu_2). \tag{A12}$$

Here $T_{\rm c}=T_{12}=T_{21}$ is the coherent transmission probability. These carriers never reach reservoir 3. Thus the total transmission probability has two terms, as indicated in Equations (1) and (2). The two-terminal conductance with the voltages (chemical potentials) measured at reservoirs 1 and 2 becomes

$$G = I/V = eI/(\mu_1 - \mu_2) = (e^2/\hbar)T_{\text{tot}}$$

$$= (e^2/\hbar)\left(T_c + \frac{S_b S_f}{S_b + S_f}\right). \tag{A13}$$

An extension of this approach for conductors with many states at the Fermi energy is discussed in [28].

For completeness, and to avoid potential misunderstanding, the expression for the conductance for the case of a sizable spread kT is added here. Assuming that reservoir j emits carriers with a Fermi distribution

$$f(E - \mu_i) = [\exp(E - \mu_i)/kT + 1]^{-1}, \tag{A14}$$

a repetition of the steps explained above yields $\mathcal{G} = \mathcal{G}_c + \mathcal{G}_i$, with

$$G_{c} = (e^{2}/\hbar) \int dE(-df/dE)T_{c}(E)$$
 (A15)

and

$$G_{i} = (e^{2}/\hbar) \frac{\int dE(-df/dE)S_{b}(E) \int dE(-df/dE)S_{f}(E)}{\int dE(-df/dE)[S_{b}(E) + S_{f}(E)]}, \quad (A16)$$

where df/dE is the derivative of the equilibrium Fermi function $f(E-E_{\rm F})$.

Appendix B: Solution of specific example

Below we present a calculation which specifies the basic ingredients of our approach, the transmission probabilities T_{ij} and the reflection probabilities R_{ij} . The barriers to the right and left of the junction (see Figure 1) are specified by 2×2 s-matrices which determine the outgoing waves in terms of the incident waves. (Alternatively, we can also specify transfer matrices.) The elements of the 2×2 s-matrix are the reflection amplitudes r_1 , r'_1 and the transmission amplitudes $t_1 = t'_1$ for the scatterer to the left and r_2 , r'_2 , t_2 for the scatterer to the right. Here the quantities without a prime give the reflection and transmission amplitudes for carriers incident from the left and the quantities with a prime give the reflection and transmission amplitudes for carriers incident from the right. These amplitudes are conveniently expressed in the form

$$t_j = T_j^{1/2} e^{i\phi_j} \tag{B1}$$

and

$$r_j = iR_j^{1/2} e^{i(\phi_j + \phi_{a,j})},$$
 (B2)

$$r'_{i} = iR_{i}^{1/2}e^{i(\phi_{j} - \phi_{a,j})},$$
 (B3)

where T_i and R_i are the transmission and reflection probability of the barrier, respectively; ϕ_i is the phase accumulated during barrier traversal; $\phi_i + \phi_{a,j}$ is the phase change associated with reflection for carriers incident from the left-hand side, and $\phi_i - \phi_{ai}$ is the phase change associated with reflection for carriers incident from the righthand side. The phase ϕ accumulated by traversing the piece of perfect wire between the two barriers can also be included in the amplitudes given above. Below we assume that the junction (triangle in Figure 1) connects precisely to the center of the well. The following substitutions in Equations (B1) - (B3) account for the phase increments for traversal from the barrier to the center of the well: $\phi_1 \rightarrow \phi_1 + \phi/2$, $\phi_{a,1} \to \phi_{a,1} - \phi/2, \ \phi_2 \to \phi_2 + \phi/2, \ \phi_{a,2} \to \phi_{a,2} + \phi/2.$ Multiplication of the two transfer matrices associated with the two scatterers yields a combined transmission probability through the double well structure given by

$$T_{12} = \frac{|t_1 t_2|^2}{|1 - r_1' r_2|^2}.$$
 (B4)

By using Equations (B1) – (B3) and the substitutions just discussed, Equation (B4) becomes [3]

$$T_{12} = \frac{T_1 T_2}{1 + R_1 R_2 + 2R_1^{1/2} R_2^{1/2} \cos(\Phi)},$$
 (B5)

where

$$\Phi = 2\phi + \phi_1 + \phi_2 + \phi_{\alpha_2} - \phi_{\alpha_1}. \tag{B6}$$

Equations (B5) and (B6) are exact. The phase accumulated in the well is

$$\phi = kw = w(2mE)^{1/2}/\hbar,$$
 (B7)

where w is the distance between the barriers and E is the energy of the incident carriers. To simplify the analysis, we assume now that it is only the energy dependence of the phase accumulated in the well which matters, and that the energy dependence of all the other amplitudes and phases in Equations (B5) and (B6) can be neglected. Thus $\Phi(E) = 2\phi(E) + \Delta\phi$, with ϕ determined by Equation (B7) and $\Delta\phi$ an energy-independent phase. Note that we are only concerned with transmission in a narrow energy interval. If only the phase ϕ accumulates during well-traversal counts, then the condition for resonance of the transmission probability [Equation (B5)] is $\Phi = 2\phi(E) + \Delta\phi = \pi(2n+1)$, where n is an integer. This condition determines the phase $\phi = \phi_{r,n}$ accumulated at resonance, and determines through Equation (B7) the resonant energy $E_{r,n}$. In the limit of

impenetrable barriers, $R_1=R_2=1$, we have $\Delta\phi=\pi$, and the resonance condition $\Phi=2\phi(E)+\Delta\phi=\pi(2n+1)$ yields the ladder of eigenstates of a square well, $E_n=(h^2\pi^2/2m)(n/w)^2$. Due to the simplifying assumption made above, the transmission probability, Equation (B5), exhibits a whole ladder of resonant states. Below we investigate the behavior of the transmission probability near one of these resonant levels. Expansion of the denominator away from $\phi=\phi_{r,n}$, for small transmission probabilities $T_1\ll 1$, $T_2\ll 1$, yields Equations (3) – (6). The transmission is minimal for $\Phi=2\pi n$, and this value is taken as a measure for the off-resonant transmission probabilities the denominator of Equation (B5) is $(1+R_1^{1/2}R_2^{1/2})^2 \approx 4$, and hence the off-resonant transmission is proportional to $\frac{1}{4}T_1T_2$ as stated in Equation (7).

Let us now specify the properties of the junction in Figure 1. The junction connects the conductor (channels 1 and 2) to the extra branch (channels 3 and 4). The amplitudes of the incoming waves in these channels (see Figure 1) are denoted by c_i and the amplitudes of the outgoing waves are denoted by c_k' . These amplitudes are related by a 4×4 scattering matrix s_{kl} such that $c_k' = \sum s_{kl}c_l$. A simple choice is [5]

$$\mathbf{s} = \begin{pmatrix} 0 & \sqrt{1-\varepsilon} & \sqrt{\varepsilon} & 0\\ \sqrt{1-\varepsilon} & 0 & 0 & \sqrt{\varepsilon}\\ \sqrt{\varepsilon} & 0 & 0 & -\sqrt{1-\varepsilon}\\ 0 & \sqrt{\varepsilon} & -\sqrt{1-\varepsilon} & 0 \end{pmatrix} . \tag{B8}$$

The parameter ε plays the role of a coupling parameter and is later related to the inelastic scattering rate. For $\varepsilon = 0$, the junction completely decouples the extra branch (channels 3 and 4) from the conductor. For $\varepsilon = 1$, carriers incident in channel 1 are transmitted into channel 3 with probability 1 and carriers incident in channel 2 are transmitted into channel 4 with probability 1. Therefore, in this limit all the carriers in the conductor approaching the junction reach reservoir 3. Some detailed results presented below do depend on the particular choice of the splitter, Equation (B8). We cannot, in general, expect results which are independent of the specific phase-randomizing mechanism. In general, all the matrix elements in Equation (B8) can be different from zero. Moreover, the matrix elements can be energydependent. As mentioned in [5], this can give rise to peaks in the conductance whose origin is not resonant transmission.

To obtain the overall transmission probabilities T_{ij} , R_{ij} for the structure shown in Figure 1, we need to determine four wave functions ψ_j . The wave function ψ_j has amplitude 1 in channel j describing incident carriers with a unit flux, and has amplitude t_{ij} describing carriers reflected into channel i and amplitude t_{ij} describing carriers transmitted into channel j. From these amplitudes the transmission and reflection

probabilities T_{ij} and R_{ij} are obtained. A calculation yields the following results:

$$R_{11} = [R_1 + (1 - \varepsilon)^2 R_2 + 2R_1^{1/2} R_2^{1/2} (1 - \varepsilon) \cos(\Phi)] / |Z|^2, \quad (B9)$$

$$R_{22} = [R_2 + (1 - \varepsilon)^2 R_1]$$

+
$$2R_1^{1/2}R_2^{1/2}(1-\varepsilon)\cos(\Phi)]/|Z|^2$$
, (B10)

$$R_{13} = \varepsilon^2 R_1 / |Z|^2, \tag{B11}$$

$$R_{44} = \varepsilon^2 R_2 / |Z|^2, \tag{B12}$$

$$R_{43} = R_{34} = [1 + R_1 R_2 + 2R_1^{1/2} R_2^{1/2} \cos(\Phi)] / |Z|^2,$$
 (B13)

$$T_{21} = T_{12} = (1 - \varepsilon)T_1T_2/|Z|^2,$$
 (B14)

$$T_{31} = T_{13} = \varepsilon T_1 / |Z|^2,$$
 (B15)

$$T_{32} = T_{23} = \varepsilon (1 - \varepsilon) T_2 R_1 / |Z|^2,$$
 (B16)

$$T_{41} = T_{14} = \varepsilon (1 - \varepsilon) T_1 R_2 / |Z|^2,$$
 (B17)

$$T_{42} = T_{24} = \varepsilon T_2 / |Z|^2,$$
 (B18)

where

$$|Z|^2 = 1 + (1 - \varepsilon)^2 R_1 R_2 + 2(1 - \varepsilon) R_1^{1/2} R_2^{1/2} \cos(\Phi).$$
 (B19)

If we allow for complex ϕ (complex energy), the amplitude $Z=1+(1-\varepsilon)R_1^{1/2}R_2^{1/2}e^{i\Phi}$ vanishes at the energy (B8) $E=E_r-i(\Gamma_{\rm e}+\Gamma_{\rm i})/2$. Here the elastic width is given by

$$\Gamma_{c} = -\hbar\nu \log(R_{1}R_{2}),\tag{B20}$$

and the "inelastic" width by

$$\Gamma_{i} = -2\hbar\nu\log(1-\varepsilon). \tag{B21}$$

For $\varepsilon=0$, when channels 3 and 4 are decoupled from the conductor we find the results discussed at the beginning of this Appendix; i.e., the results for T_{12} given by Equations (B5) and (B14) are the same, and $R_{11}=R_{22}=1-T_{12}$. The Breit and Wigner formulae [1, 2] (see also Appendix C) are obtained from Equations (B9) – (B18) in the limit $O(\varepsilon)=O(T_1)=O(T_2)\ll 1$, with the partial widths given by Equations (6) and (13). The total elastic and inelastic widths are consistent with Equations (B20) and (B21) in the limit of small transmission probability and small ε . The results of Section 4, the limit of ε close to 1, are obtained by expanding Equations (B14) – (B18) to first order in $(1-\varepsilon)$. Equation (B21) allows an interpretation of the parameter ε in terms of an inelastic scattering time; with $\Gamma_i=\hbar/\tau_i$ we obtain from Equation (B21)

$$\varepsilon = 1 - e^{-1/2\nu\tau_i}. ag{B22}$$

From Equations (B15) – (B18) we obtain for the forward and backward scattering rates

$$S_{\rm b} = \varepsilon T_1 [1 + (1 - \varepsilon)R_2]/|Z|^2, \tag{B23}$$

$$S_{\rm f} = \varepsilon T_2 [1 + (1 - \varepsilon)R_1]/|Z|^2.$$
 (B24)

Together with $T_{\rm c}=T_{12}$, with T_{12} given by Equation (B14), Equations (B23) and (B24) determine the total transmission probability $T_{\rm tot}$, Equation (1), for arbitrary coupling ε . Figures 2(a) and 2(b) are generated with the help of these results.

Appendix C: The Breit and Wigner formulae

The Breit and Wigner formulae determine the scattering matrix in the presence of a resonance. They are usually derived in the context of nuclear reactions [1, 2] and this perhaps accounts for the fact that they seem not to be appreciated in solid-state physics. Consider a barrier connected to two perfect wires [4, 29]. In the perfect wires the longitudinal motion is assumed to be separable from the transverse motion. Thus motion in narrow perfect wires can be characterized by the quantized motion in the transverse direction, giving rise to a set of discrete energies E_r Kinetic longitudinal energy can be added to the transverse energy to give the Fermi energy: $E_F = \hbar k_i^2 / 2m + E_i$. Here we have used a free-particle term to characterize the kinetic energy of the longitudinal motion, but this is not essential. Thus each channel j is associated with two states at the Fermi level with longitudinal velocities $v_i = \pm \sqrt{(2/m)(E_F - E_i)}$. We have N input channels and N output channels. The set of transverse energies in the perfect wire to the left of the barrier can be equal to or different from the set of transverse energies to the right of the barrier. Similarly, for conductors with side branches, we assign a set of channels to each branch of the conductor [5, 22, 28]. For the conductor of Figure 1, N = 4. The conducting sample mixes these channels; i.e., a wave incident in channel j leads in general to outgoing waves in all the channels. We have used here the notion of channels in a perfect conductor [29] as an example. The Breit and Wigner formulae presented below apply quite independently of the particular properties of the channels, i.e., whether we deal with plane waves, Bloch waves, or spherical waves. Let us denote the amplitude of the incident current in channel j by a_i and the outgoing current amplitude in channel j by a'_i . The relation between the incoming waves and the outgoing waves is given by an s-matrix $a_i' = \sum_{j=1}^{j=N} s_{ij} a_j$. Current conservation requires the matrix s to be unitary, and time reversal (in the absence of a magnetic field) requires in addition that this matrix be symmetric, $s_{ii} = s_{ii}$. Suppose now that the barrier contains a state with a long lifetime h/Γ at an energy $E = E_r - i\Gamma/2$. The key point of Breit and Wigner is the following: All matrix elements of the s-matrix which relate to the decay of the resonance must themselves be resonant and have a denominator of the form $E - E_r + i\Gamma/$ 2. Below we assume that all the channels of the s-matrix discussed above couple to the resonant state. If this is not the case, our considerations apply to a properly defined and reduced portion of the s-matrix. The s-matrix takes an especially simple form if it is expressed on the basis of the "eigenchannels" which are related to the channels discussed above by an orthogonal transformation O. Consider for

simplicity a sample (barrier) connected to only two perfect wires. The eigenchannels are defined in the following way: Away from the resonant energy, transmission through the sample is very small and can be neglected. Thus, away from resonance, carriers incident on the sample are (in this approximation) totally reflected. In general, carriers incident in channel j are reflected with nonvanishing probabilities into all the channels of the perfect conductor. The eigenchannels are chosen such that the reflection away from resonance is diagonal. There is an orthogonal transformation O₁ which transforms the channels of the left perfect conductor and an orthogonal transformation O, which transforms the channels of the right perfect conductor. On the basis of eigenchannels the s-matrix away from resonance is given by $s_{mn} = \delta_{mn} e^{i(\delta_m + \delta_n)}$, where δ_{mn} is the Kronecker symbol and δ_m are the phases acquired in the reflection process. On the basis of the eigenchannels, and in the presence of resonant transmission, the matrix elements of the s-matrix are of the form

$$s_{mn} = \left[\delta_{mn} - i \frac{\Gamma M_{mn}}{E - E_{\rm r} + i\Gamma/2}\right] e^{i(\delta_m + \delta_n)},\tag{C1}$$

where the matrix elements M_{nm} remain to be determined. The s-matrix is symmetric, and hence $M_{mn} = M_{nm}$. Furthermore, since s is unitary, differing rows of the s-matrix must be orthogonal to one another. The orthogonality of rows m and n gives

$$\frac{M_{mn}^{*}}{E - E_{r} - i\Gamma/2} - \frac{M_{mn}}{E - E_{r} + i\Gamma/2} = \frac{i\Gamma \sum_{j=1}^{j=N} M_{mj} M_{nj}^{*}}{(E - E_{r})^{2} + \frac{1}{4} \Gamma^{2}}.$$
(C2)

As shown in [2], Equation (C2) implies first that M_{mn} is real and second that M_{nm} is a matrix which is equal to its own square. Since \mathbf{M} is symmetric, it can be diagonalized, and since the matrix is unimodular, its eigenvalues are either 0 or 1. If there is no accidental degeneracy of resonant levels in the sample, all eigenvalues of the \mathbf{M} -matrix are equal to 0 except for one eigenvalue, which is equal to 1. As shown in [2], in this case

$$M_{mn} = \sqrt{\Gamma_m \Gamma_n} / \Gamma, \tag{C3}$$

where the Γ_m are called the *partial widths* of the channels and $\Gamma = \sum_{j=1}^{j=N} \Gamma_j$ is the total width of the resonant level. Thus the set of phases δ_n , $n=1, \dots, N$, and the N partial widths determine the matrix elements of the s-matrix. The matrix [Equation (C1)] specified by Equation (C3) is unitary. The constraint $\sum_{n=1}^{n=N} \delta_n = \delta$, where $\sin \delta = \Gamma/2[(E-E_r)^2 + (\Gamma/2)^2]^{1/2}$, makes s_{mn} a special unitary matrix. Using Equations (C3) and (C1) yields a probability

$$S_{mn} = |s_{mn}|^2 = \frac{\Gamma_m \Gamma_n}{(E - E)^2 + \frac{1}{2} \Gamma^2}$$
 (C4)

for $m \neq n$ and

$$S_{nn} = |s_{mn}|^2 = \frac{(E - E_r)^2 + \frac{1}{4} (\Gamma - \Gamma_n)^2}{(E - E_r)^2 + \frac{1}{4} \Gamma^2}$$
 (C5)

for n = m. Thus the Breit and Wigner formulae, Equations (C4) and (C5), determine the transmission probabilities and the reflection probabilities of a resonant scatterer coupled to N channels in terms of the partial widths of these channels. For the particular example analyzed in Appendix B, we find that in the Breit and Wigner limit, Equations (B11), (B12), and (B14) – (B18) are of the form given by Equation (C4), and Equations (B9), (B10), and (B13) are of the form given by Equation (C5). In this example the transformation to eigenchannels affects only channels 3 and 4.

As an additional application of these results, let us consider the case of a single resonant well in a barrier connected to the left and right to perfect wires (see [16] and [17]). The perfect wire to the left has N_i quantum channels, and the perfect wire to the right has N_r quantum channels. The total number of channels is $N = N_r + N_r$. The decay into the eigenchannels on the left-hand side of the barrier gives rise to the partial widths Γ_{ij} and the decay into the eigenchannels on the right-hand side gives rise to the partial widths $\Gamma_{r,i}$. The probability for transmission from channel j (on the l.h.s.) to channel i (on the r.h.s.) is, according to Equation (C4), $T_{ij} = \Gamma_{r,i}\Gamma_{\lambda,j}/(E - E_r)^2 + \frac{1}{4}\Gamma^2$. Here $\Gamma = \Gamma_r + \Gamma_r$ is the total width and $\Gamma_r = \sum_{i=1}^{i=N_r} \Gamma_{r,i}$ is the total partial width associated with decay of the resonant state into the r.h.s. perfect conductor, and $\Gamma_{\ell} = \sum_{j=1}^{j=N_{\ell}} \Gamma_{\ell,j}$ is the total width associated with the decay into the l.h.s. perfect conductor. The conductance [29, 32]

$$G = \left(\frac{e^2}{\hbar}\right) \operatorname{tr}(t^+ t) = \left(\frac{e^2}{\hbar}\right) \sum_{i=1, i=1}^{i=N_{r,j}=N_f} T_{ij}$$

is easily evaluated and given by

$$G = \left(\frac{e^2}{\hbar}\right) \frac{\Gamma_r \Gamma_r}{\left(E - E_r\right)^2 + \frac{1}{4} \left(\Gamma_r + \Gamma_r\right)^2}.$$
 (C6)

Here we have evaluated the conductance on the basis of eigenchannels, which is allowed since $\operatorname{tr}(t^+t)$ is invariant under the orthogonal transformations O_r and O_r discussed above. Thus, application of the Breit and Wigner formulae immediately yields the key result of Kalmeyer and Laughlin [17]. In the presence of a single resonant state the conductance is bounded by e^2/\hbar . The maximum value is obtained if $\Gamma_r = \Gamma_r$. A single resonant state, described in the Breit and Wigner formalism by requiring that the M-matrix have only one eigenvalue equal to 1, can at best provide one effective conduction channel [33].

Appendix D: Local density of states

In this section we discuss the density of states in the well and the effect of inelastic scattering on the density of states. Let x be the coordinate along the conductor, with x = 0 marking

the location of the junction. The number of carriers in the segment of the conductor between x and x + dx and in an energy interval E, $E + \Delta E$ due to carriers incident in channel j is [24, 31]

$$dN(x) = (dn/dE)\Delta E |\psi_i(E, x)|^2 dx.$$
 (D1)

Here $(dn/dE) = 1/2\pi\hbar v$ is the density of states in channel j. The wave function is normalized such that the incident wave has amplitude 1. In the conductor of Figure 1 we have a total of four wave functions, each describing carriers incident in one of the four channels. Thus, in the sample of Figure 1, assuming that the density of states of all the channels is the same, the number of carriers in an interval from x to x + dx is given by

$$dN(x) = (dn/dE)\Delta E \sum_{j=1}^{j-4} |\psi_j(E, x)|^2 dx.$$
 (D2)

Let us now apply Equation (D2) to find the total number of carriers in the resonant well. This requires that we integrate the right-hand side of Equation (D2) over the width of the well. Dividing this by ΔE yields the number of states in the well per unit energy,

$$dN/dE = (dn/dE) \sum_{k=1}^{k=4} \int_{x=-w/2}^{x=w/2} dx |\psi_k(E, x)|^2.$$
 (D3)

For a well which is wide compared to the Fermi wavelength, the integration limits are determined by the turning points. We are not interested in density variations on the scale of a Fermi wavelength and, therefore, it is sufficient to use a density which has been averaged over a small volume several times larger than the scale set by the Fermi wavelength [3, 24, 29, 31]. In the well the wave function is a superposition of plane waves. The averaged square of the wave function to the left (and right) of the splitter is determined by a pair of amplitudes, a_2 , a'_2 , b_1 , b'_1 , respectively. For instance, the averaged wave functions to the left of the splitter are given by $\langle |\psi_i(x)|^2 \rangle = |a_2(j)|^2 +$ $|a'_{i}(j)|^{2} = |c_{i}(j)|^{2} + |c'_{i}(j)|^{2}$. Here the $\langle \rangle$ indicate the spatial average. Because the a and c coefficients (see Figure 1) in this equation differ only by phase factors, either set can be used. For brevity we do not present this calculation in detail but only give the final result,

 $dN/dE = (dn/dE)(w/2)(1/|Z|^2)$

$$\times [(2 - \varepsilon)(T_1 + T_2) + (1 - \varepsilon)(2 - \varepsilon)(R_1T_2 + R_2T_1)$$

$$+ 2\varepsilon + \varepsilon(2 - \varepsilon)(R_1 + R_2) + 2\varepsilon(1 - \varepsilon)R_1R_2].$$
 (D4)

The number of states per unit energy, Equation (D4), is shown in Figure 3. Equation (B7) is used to obtain the energy dependence. In the Breit and Wigner limit, Equation (D4) yields Equation (17). In the limit $\varepsilon = 1$ corresponding to complete phase randomization, the density of states in the well is the same as that in the perfect leads connecting to the reservoirs; i.e., Equation (D4) yields dN/dE = (dn/dE)2w. Clearly, for a narrow well with a width of the order of the

Fermi wavelength, the approximations used above to find the number of states in the well are not adequate. The key point of our discussion, already made in [24], is that inelastic scattering affects the density of states.

References and notes

- 1. G. Breit and E. Wigner, Phys. Rev. 49, 519 (1936).
- L. D. Landau and E. M. Lifshitz, Quantum Mechanics (Non-Relativistic Theory), Pergamon Press, Oxford, 1977. See p. 603 ff.
- 3. R. Landauer, *IBM J. Res. Develop.* 1, 223 (1957); R. Landauer, *Philos. Mag.* 21, 863 (1970).
- R. Landauer, "Electrical Transport in Open and Closed Systems," Z. Phys. B 68, 217 – 228 (1987).
- 5. M. Büttiker, Phys. Rev. B 33, 3020 (1986).
- E. O. Kane, Tunneling Phenomena in Solids, E. Burnstein and D. Lundquist, Eds., Plenum Press, New York, 1969.
- R. Tsu and L. Esaki, Appl. Phys. Lett. 22, 562 (1973);
 L. L. Chang, L. Esaki, and R. Tsu, Appl. Phys. Lett. 24, 593 (1974).
- T. C. L. Sollner, W. D. Goodhue, P. E. Tannenwald,
 C. D. Parker, and D. D. Peck, Appl. Phys. Lett. 43, 588 (1983).
- 9. R. Ricco and M. Ya. Azbel, Phys. Rev. B 29, 1970 (1984).
- 10. S. Luryi, Appl. Phys. Lett. 47, 490 (1985).
- 11. P. J. Price, Superlattices and Microstructures 2, 593 (1986).
- F. Capasso, K. Mohammed, and A. Y. Cho, *IEEE J. Quant. Electron.* **QE-22**, 1853 (1986).
- E. Mendez, L. Esaki, and W. I. Wang, *Phys. Rev. B* 33, 2893 (1986).
- 14. T. Weil and B. Vinter, Appl. Phys. Lett. 50, 1281 (1987).
- 15. P. J. Price, Phys. Rev. B 33, 1314 (1987).
- H. Knauer, J. Richter, and P. Seidel, *Phys. Status Sol. (a)* 44, 303 (1977); A. Hartstein and R. H. Koch, *Phys. Rev. B* 35, 6442 (1987)
- 17. V. Kalmeyer and R. B. Laughlin, Phys. Rev. B 35, 9805 (1987).
- M. Ya. Azbel, A. Hartstein, and D. P. DiVincenzo, *Phys. Rev. Lett.* 52, 1641 (1984).
- 19. A. D. Stone and P. A. Lee, *Phys. Rev. Lett.* **54**, 1196 (1985).
- A. B. Fowler, G. L. Timp, J. J. Wainer, and R. A. Webb, *Phys. Rev. Lett.* 57, 138 (1986).
- N. D. Lang, *Phys. Rev. Lett.* 58, 45 (1986); "The Resistance of a One-Atom Contact in the Scanning Tunneling Microscope," preprint.
- 22. M. Büttiker, Phys. Rev. Lett. 57, 1761 (1986).
- M. Büttiker, Y. Imry, and R. Landauer, *Phys. Lett.* 96A, 365 (1983).
- M. Büttiker, Phys. Rev. B 32, 1846 (1985); Ann. N.Y. Acad. Sci. 480, 194 (1986).
- H. Morkoç, J. Chen, U. K. Reddy, T. Henderson, and S. Luryi, *Appl. Phys. Lett.* 49, 70 (1986).
- 26. The results of [5] are expressed in terms of the Landauer formula $R_L = (h/e^2)(1 T_{tot})/T_{tot}$. This differs from the two-terminal conductance used here by a "contact resistance" h/e^2 . See Y. Imry in *Directions of Condensed Matter Physics*, (Memorial Volume in Honor of Shang-keng Ma), G. Grinstein and G. Mazenko, Eds., World Scientific Press, Singapore, 1986, and [4].
- 27. We assume here that inelastic scattering in the well is the dominant effect. If the inelastic scattering time is short compared to the single-barrier traversal time [see M. Büttiker and R. Landauer, *Phys. Rev. Lett.* 49, 1739 (1982); C. R. Leavens and G. C. Ares, *Solid State Commun.* 62, 1101 –1105 (1987)], inelastic effects during barrier traversal must be taken into account.
- 28. M. Büttiker, Phys. Rev. B 35, 4123 (1987).
- M. Büttiker, Y. Imry, R. Landauer, and S. Pinhas, *Phys. Rev. B* 31, 6207 (1985).
- H. L. Engquist and P. W. Anderson, *Phys. Rev. B* 24, 1151 (1981).

- O. Entin-Wohlman, C. Hartzstein, and Y. Imry, *Phys. Rev. B* 34, 921 (1986).
- 32. D. S. Fisher and P. A. Lee, *Phys. Rev. B* 23, 6851 (1981).
- 33. Y. Imry, Europhys. Lett. 1, 249 (1986).
- 34. J. Jonson and A. Grincwajg, "The Effect of Inelastic Scattering on Resonant and Sequential Tunneling in Double Barrier Heterostructures," preprint; available from authors, Institute of Theoretical Physics, Chalmers University of Technology, Göteborg, Sweden.

Received September 11, 1987; accepted for publication September 20, 1987

Markus Büttiker IBM Thomas J. Watson Research Center, P.O. Box 218, Yorktown Heights, New York 10598. Dr. Büttiker is a research staff member of the Physical Sciences Department at the Thomas J. Watson Research Center. He is currently conducting research in coherent transport phenomena in ultrasmall metallic structures. He received a Diploma in theoretical physics from the Federal Institute of Technology in Zurich, Switzerland, in 1974, and a Ph.D from the University of Basel, Switzerland, in 1978. He joined IBM at the Thomas J. Watson Research Center in 1979. Dr. Büttiker's research interests include such diverse fields as current instabilities in semiconductors, the statistical mechanics of solitons, and thermal activation and nucleation phenomena.